Preprint Title Understanding the Aggregation-Induced Emission Mechanisms Originated from Phenoxazine and Phenothiazine Groups

Authors Ying Gao, Yanchun Liu and Yong Wu

Publication Date 24 Nov 2023

Article Type Full Research Paper

ORCID® iDs Ying Gao - https://orcid.org/0000-0002-3083-8555

Understanding the Aggregation-Induced Emission Mechanisms Originated from Phenoxazine and Phenothiazine Groups

Ying Gao, Yan-Chun Liu*, Yong Wu

[a.] Jilin Provincial Key Laboratory of Straw–Based Functional Materials, Institute for Interdisciplinary Biomass Functional Materials Studies, Jilin Engineering Normal University, Changchun 130052, China

[b.] Key Laboratory of Electrochemical Energy Storage and Energy Conversion of Hainan Province, School of Chemistry & Chemical Engineering, Hainan Normal University, Haikou 571158, China.

[c.] Faculty of Chemistry, Northeast Normal University, Changchun, Jilin 130024, China

Abstract

Four molecules bearing carbazole (**Cz**), phenoxazine (**PXZ**) and phenothiazine (**PTZ**) as donor groups to diphenylsulfone acceptor have been reported. Molecule containing **Cz** just shows thermally activated delayed fluorescence (TADF) property, but molecules containing **PXZ** and **PTZ** display TADF and aggregation-induced emission (AIE) properties. In this work, a thorough investigation was done on four molecules in order to resolve the AIE mechanism originated from **PXZ** and **PTZ** groups. The combination of molecular dynamics and quantum chemistry study indicates that the AIE property of **DPS-PTZ** is originated from the reason that the environment of thin film restricts the molecular twist, decreases the non-radiative decay and leads to the AIE property for **DPS-PTZ**. For **DPS-PXZ**, the quantum chemistry result indicates that the decay path from the single excited state (S_1) leading to a conical interaction (CI) via enlarging the C-S-C angle is the key factor for possessing AIE property. The **DPS-PXZ** follow the restricted access to a CI (RACI) model because that the twist must be blocked in the aggregate state, inhibiting the decay and leading to luminescence. Discovering the wording mechanism is beneficial for providing design guidelines for the development of new AIE systems for new practical applications.

Key words：thermally activated delayed fluorescence; aggregation-induced emission; conical interaction; molecular dynamics; quantum chemistry

1. Introduction

The optimization of organic light emitting diode (OLED) technologies has challenged chemists since Tang and Van Slyke firstly reported OLED in 1987. [1] Seeing the history of OLED materials, the purely organic materials with delayed fluorescence (DF) theoretically endow 100% internal quantum efficiency owing to the small singlet–triplet energy splitting (ΔE_{ST}) and efficient up-conversion of triplet exciton (75%) into singlet exciton. [2-4] Considering the OLED applications, the efficiency is a thorny problem, in which the aggregation-concentration quenching (ACQ) effect is always happen when the luminophores are used in the aggregate state as thin solid films. [5, 6]

In 2001, Tang and co-workers occasionally observe that a solution of 1-methyl-1,2,3,4,5-pentaphenylsilole in ethanol shows a strong increase in fluorescence with an addition of water, which is termed as aggregation-induced emission (AIE). Different from the conventional chromophores, the luminogens with AIE can effectively surmount the universal ACQ problem, whose emissions are enhanced by aggregation. [7] Later, the application of AIE phenomenon was strongly advanced by Tang group as witnessed by a remarkable number of reviews. [8-10] Since the AIE term was proposed, various hypotheses have been suggested on AIE mechanisms, such as restriction of intramolecular motion (RIM), [11-15] restricted access to a conical intersection (RACI), [16] excimer formation, J-aggregates, [17] twisted intramolecular charge transfer (TICT) state, [18, 19] and excited state intramolecular proton transfer (ESIPT). [20] Thanks to the enthusiastic efforts of scientists worldwide, many AIEgens based on RIM mechanism have been developed, such as tetraphenylethene (TPE), tetraphenylpyrazine (TPP), [21] silole, [22] quinoline-malononitrile (QM), [23] cyanostilbene, [24] 9,10-distrylanthracene (DSA), [25] and organoboron complexes. [26]

The active intramolecular motion in solution will be restricted in aggregate or the solid state could be demonstrated by many experimental results. To restrict the molecular motions, the common methods is incorporating the chromophores into a

high viscosity medium, lowering the temperature, doping them in rigid polymer matrix or embedding them into metal organic frameworks. [27-31] These molecules always possess electron donor and electron acceptor unites, implying that the properties of electronic states are affected strongly by the solvent polarity. The time-resolved fluorescence spectra indicates that the efficient occurrence of AIE is from eliminated intramolecular charge transfer (ICT) state due to the gradual transition from local excited (LE) state to ICT with increasing solvent polarity. Consequently, the AIE mechanism is induced by the restriction of the torsional motion of the molecules and by the restriction of the transition from the LE state to the ICT state. [32] The AIE mechanism is also the inhibition of the nonradiative channel, that is, the vibrational/torsional energy relaxation process that is blocked in aggregate state. The study on the boron dipyrromethene (BODIPY) derivatives suggest the restricted TICT. [33]

Molecular engineering endowing TADF and AIE characteristics should be a promising strategy to achieve efficient non-doped OLEDs with reduced efficiency roll-off and simple fabrication process. [34] AIE emission materials have excellent solid-state emission by suppressing concentration quenching and exciton annihilation, while TADF materials are able to fully utilize electrogenerated single and triplet excitons. Therefore, the collaboration of AIE and TADF should be a rational strategy to design novel robust luminescent materials. The AIE-TADF phenomena is quite surprising experimental findings, to date, RIM has been recognized as the general working mechanism of AIE, [35] but the underlying mechanisms of some AIE systems still remain unclear. Some works has been devoted to determining the AIE mechanism by theoreticians and experimentalists.

To date, many groups have reported the successful cases of the combination of prominent TADF and AIE properties. [36-41] In order to deepen the working mechanism of AIE-TADF, the structure difference between typical AIE-TADF and TADF should be understood. The introduction of various donor and acceptor combinations on the bridge structure is compatible with both AIE and TADF properties. A series of structurally identical luminogens (Figure 1) with a D-A

framework have been investigated using density functional theory method. Four molecules bearing carbazole (**Cz**), phenoxazine (**PXZ**) and phenothiazine (**PTZ**) as donor groups to diphenylsulfone acceptor have been reported. [37] We found that only changing one donor unit lead to dramatic property difference: some molecules display both TADF and AIE properties, whereas some molecule just possesses TADF property. In the following section, a series of properties have been calculated to investigate the property difference among them.

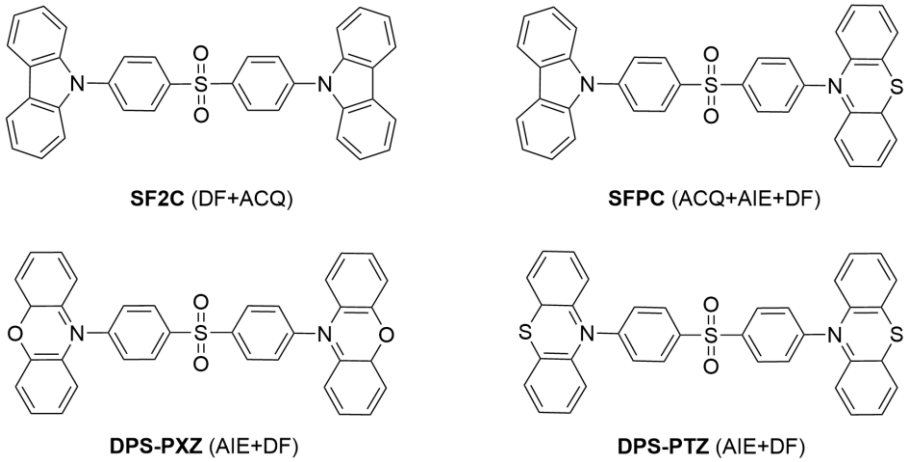

Figure 1. Molecular structures of **SF2C**, **SFPC**, **DPS-PXZ** and **DPS-PTZ**.

2. Computational details

In this work, the ground-state (S_0) geometry was optimized using density functional theory (DFT) with M062X method at the basis set level of Def2SVP. The singlet excited-stated (S_1) and triplet excited-stated (T_1) geometries were optimized using the time-dependent DFT (TD-DFT) method and unrestricted DFT (UDFT) at the same functional and basis set. Based on the equilibrium structures, frequency calculations were carried out to ensure that the optimized geometries were minima on the potential energy surface, in which no imaginary frequencies were observed in any of the molecules. In all calculations, the SMD was taken into account to considering the solvent effect. The calculations mentioned-above were performed by Gaussian16 program. In order to depict the structural variation upon electron excitation, the root mean square deviation (RMSD) between S_0 and S_1 for all molecules were obtained by

VMD program. Further to study the mechanism of luminescence, the spin-orbit coupling (SOC) constant, minimum energy crossing point (MECP) and conical interaction (CI) structures were calculated by ORCA program. At last, to simulate the aggregate phase, the GROMACSS program is employed in molecular dynamics for the investigation of the AIE mechanism originated **PXZ** and **PTZ** groups. Both gas phase and solvent dynamics were computed for **SF2C**, **SFPC**, **DPS-PXZ** and **DPS-PTZ**.

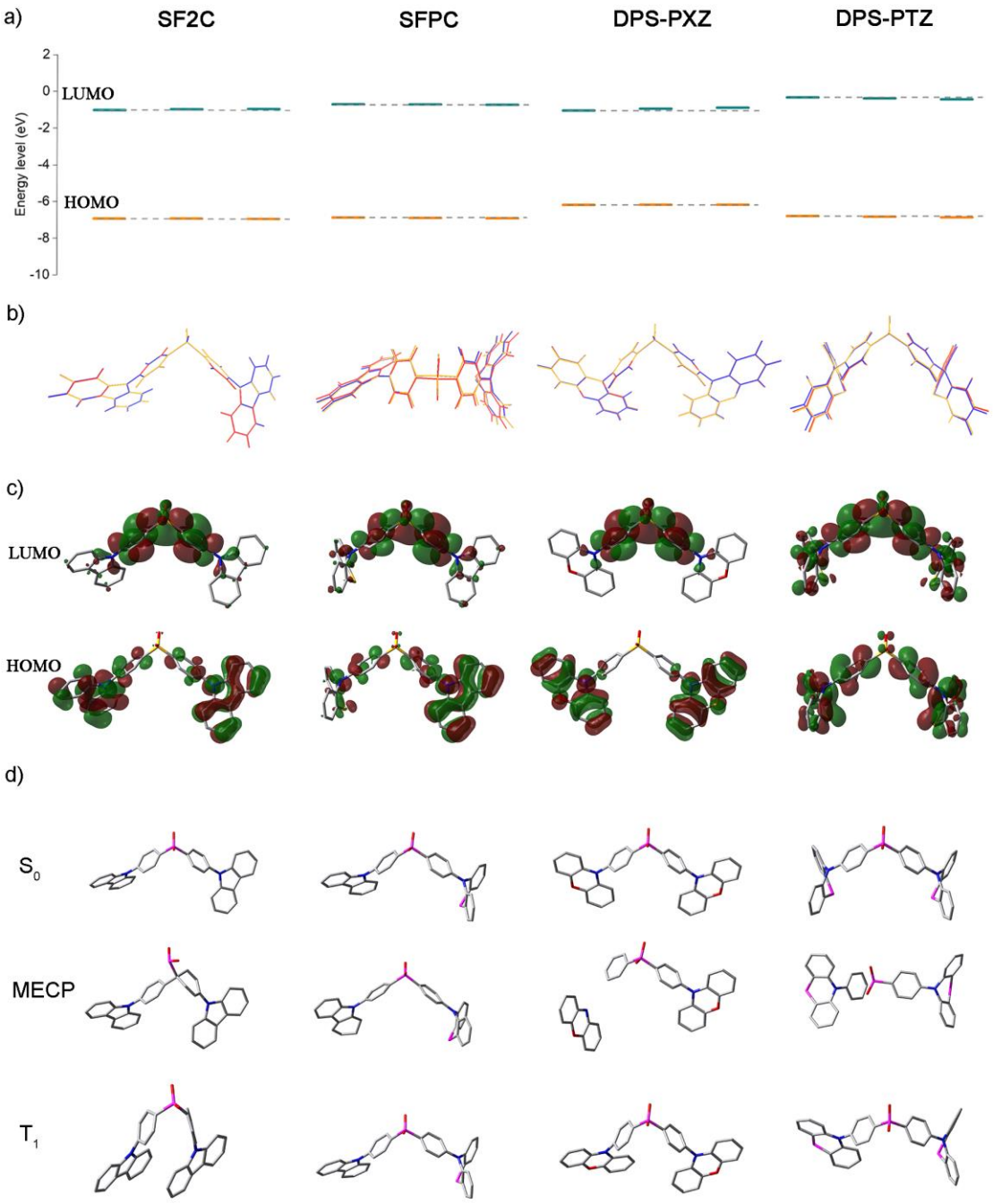

Figure 2. (a) Calculated frontier molecular orbital distributions (HOMO and LUMO) and energy levels of **SF2C**, **SFPC**, **DPS-PXZ** and **DPS-PTZ** in TOL, THF and DMSO solvents. (b) A comparison among ground-stated (S_0) structures of **SF2C**, **SFPC**, **DPS-PXZ** and **DPS-PTZ** in TOL (orange), THF (blue) and DMSO (red) solvents. (c) HOMO and LUMO distributions of **SF2C**, **SFPC**, **DPS-PXZ** and **DPS-PTZ** in TOL solvent. (d) The optimized S_0, MECP and T_1 structures of **SF2C**, **SFPC**, **DPS-PXZ** and **DPS-PTZ** in TOL solvent.

3. Results and discussions

To gain in-depth insight into the electronic structures of **SF2C**, **SFPC**, **DPS-PXZ** and **DPS-PTZ**, the geometric optimizations in TOL, THF and DMSO solvents were performed using DFT method. In the S_0 state, the **Cz** and **PXZ** are planar and rigid configuration, but the **PTZ** is bonding structure because of a sulfur bridge linking two phenyl rings forming a six-membered ring between two phenyl units. The **PTZ** moiety in the S_0 possesses a nonplanar "butterfly-like" structure with a C-C-S-N dihedral angle of about 35°. Further, based on the optimized S_0 structures, the HOMO and LUMO energy levels in TOL, THF and DMSO solvents were calculated and shown in Figure 2a. The types of solvent have a slight influence on the HOMO and LUMO energy levels of **SFPC** and **SF2C**. The LUMO of **DPS-PXZ** and **DPS-PTZ** are increased and decreased, respectively, with increasing solvent polarity. Figure 2b depicts the S_0 structural comparison in TOL, THF and DMSO solvents. The structures of **SF2C** and **DPS-PXZ** are almost unchanged in TOL, THF and DMSO solvents because that **PXZ** group possesses the planar and rigid configuration. However, the bonding structure of **PTZ** experiences a quite remarkable change with ranging solvent polarity, especially for **SFPC**.

According to the above discussions, the S_0 geometry seldom changed as the solvent polarity increased, thus implying a rather small frontier molecular orbital change in different solvent. Figure 2c depicts the HOMO and LUMO distributions. It can be seen that the HOMO and LUMO distributions are very similar for each molecule in TOL, THF and DMSO solvents. For **SF2C**, **SFPC** and **DPS-PXZ**, it can be seen that their HOMO is mainly spread over the electron-donating (**PXZ** and **PTZ**) groups, while the LUMO is primarily distributed over diphenylsulfone acceptor, displaying a better HOMO and LUMO separation. While, the HOMO and LUMO distributions of **DPS-PTZ** present a dominating delocalization on the whole molecular bone in accordance with large HOMO and LUMO overlap.

The S_0, T_1 and MECP structures between S_0 and T_1 were depicted in Figure 2d. It can be seen that the S_0 and T_1 structures of **SFPC**, **DPS-PXZ** and **DPS-PTZ** change

very little. For example, the donor and acceptor moieties of **DPS-PXZ** were almost perpendicular each other as can be ascertained in the geometrical structure in Figure 2d. For **SF2C**, **SFPC**, **DPS-PXZ** and **DPS-PTZ**, the MECP structure is unreasonable to realize. For example, the one-side **PXZ** group of **DPS-PXZ** in MECP structure happen to dissociate, and the benzene of diphenylsulfone for **DPS-PTZ** in MECP structure is broken. These observations thus clearly demonstrate that the failure of MECP is beneficial for ensuring the T_1 population and facilitating reverse intersystem crossing (RISC) from T_1 to S_1 for **SF2C**, **SFPC**, **DPS-PXZ** and **DPS-PTZ**.

Table 1 Calculated ΔE_{ST}, SOC and RMSD of **SF2C**, **SFPC**, **DPS-PXZ** and **DPS-PTZ** in TOL, THF and DMSO solvents.

ΔE_{ST}/eV	**SF2C**	**SFPC**	**DPS-PXZ**	**DPS-PTZ**
TOL	0.289	0.536	0.247	0.335
THF	0.367	0.496	0.464	0.334
DMSO	0.536	0.471	0.578	0.333
SOC/cm^{-1}	**SF2C**	**SFPC**	**DPS-PXZ**	**DPS-PTZ**
TOL	0.226	0.291	0.824	0.028
THF	0.226	0.306	0.816	0.000
DMSO	0.142	0.293	0.846	0.014

Further study listed in Table 1 has focused on ΔE_{ST}, SOC and RMSD. The calculated results indicate that the small ΔE_{ST} is beneficial for TADF emission. It can be seen that the ΔE_{ST} is associated with the type of solvent. For example, with increasing solvent polarity, the ΔE_{ST} values of **SF2C** and **DPS-PXZ** are increased, but the ΔE_{ST} values of **SFPC** and **DPS-PTZ** are decreased. The type of solvent has negligible influence on SOC values. For example, the SOC values of **SFPC** are 2.191, 0.306 and 0.293 cm^{-1} in TOL, THF and DMSO solvents, respectively. The SOC values of **DPS-PTZ** are close to zero.

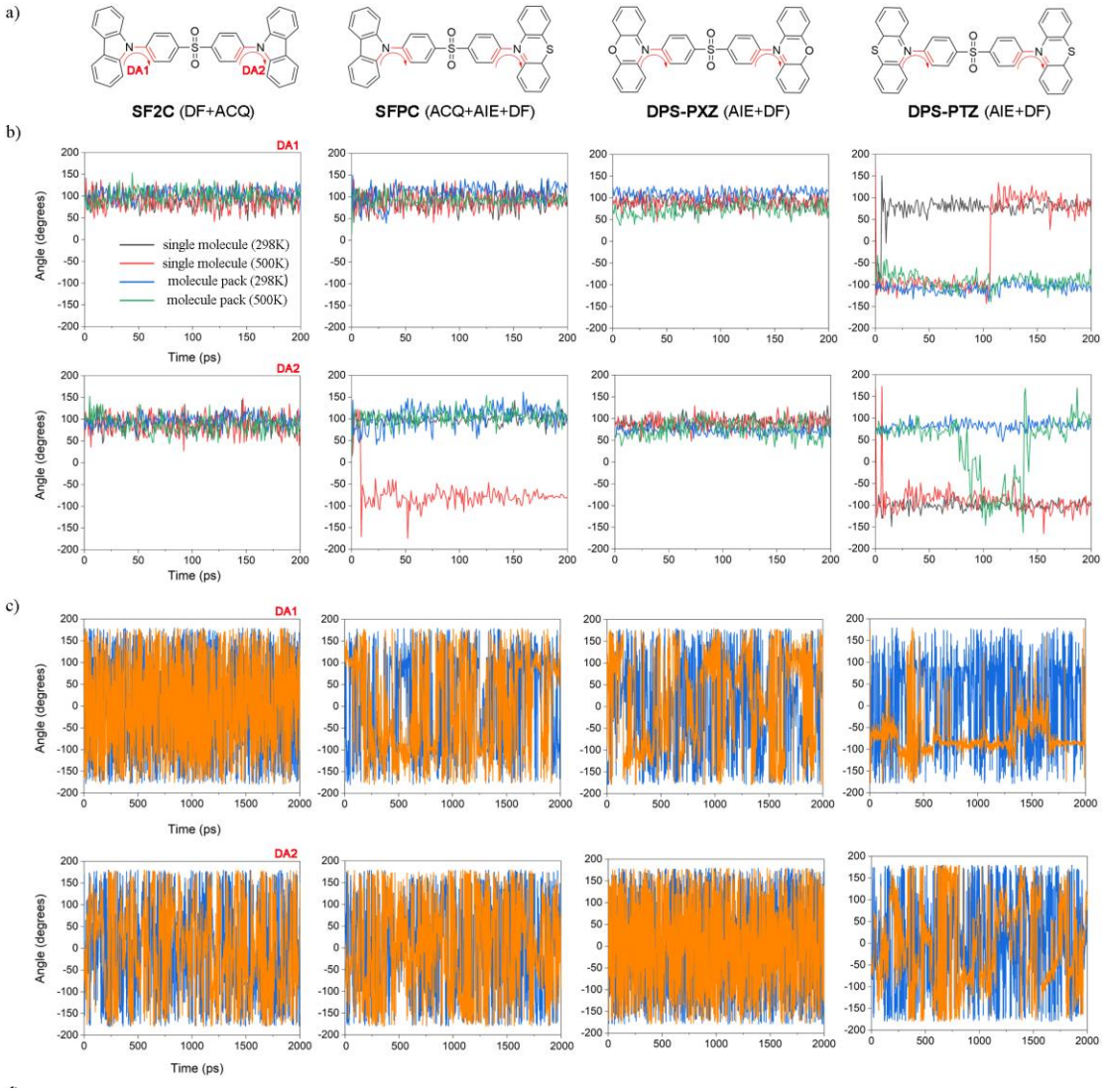

Figure 3 (a) Molecular structures of **SF2C**, **SFPC**, **DPX-PXZ** and **DPS-PTZ**. (b) Plots of DA1 and DA2 angles for single molecules and three hundred molecular cluster as a function of time. (c) Plots of DA1 and DA2 angles for boxes containing two hundred solvents and five (in blue) or thirty-five (in yellow) target molecules as a function of time.

These molecules contain the same diphenylsulfone acceptor and different **Cz**, **PXZ** and **PTZ** donor groups. However, only changing one donor unit leads to their dramatic property difference. To better understand the mechanisms of such intriguing AIE phenomena, we have carried out the molecular dynamics study on the single molecule and the aggregate state, respectively. For these molecules in a donor and acceptor model, the geometry variation after electron excitation is generally assigned to the dihedral angle between the donor and acceptor units.

Firstly, we have investigated the dihedral angles (DA1 and DA2) changes of the

single molecules and three hundred molecule cluster at 298K and 500K (Figure 3b). As for **SF2C** and **DPS-PXZ** in the single or in the aggregate state, the DA1 and DA2 have a small change no mater at 298K or 500K. The same conclusion is found for DA1 of **SFPC**. However, the DA2 of **SFPC** in the single molecule experience remarkable variation with temperature changing from 298K to 500K. It can be found that the DA2 of **SFPC** in single molecule is strongly affected by temperature, whereas the DA2 of **SFPC** in aggregate state undergo relatively small change. It is the reason that the surrounding molecules of **SFPC** cluster tend to restrict the rotation of DA2, and avoid the nonradiative decay channel. At 298K, the DA1 of **DPS-PTZ** in single molecule is in a small-range fluctuation. When it is 500K, the DA1 of **DPS-PTZ** in single molecule is in a large decrease from 0 ps to 100 ps, it then tends to the stable point from 100 ps to 200 ps. However, the DA1 of **DPS-PTZ** in aggregate state at 298K and 500K are similar and fluctuated in a small range, indicating that raising temperature has no effect on the dihedral angle between donor and acceptor groups. When the temperature is increased to 500K, the DA2 of **DPS-PTZ** in aggregate state experience a remarkable change. The calculated results indicate that the temperature and surrounding environment have less influence on the **Cz** and **PXZ** than **PTZ**. In view of geometry, the **Cz** and **PXZ** are planar and rigid configurations. However, the effect of temperature and environment have huger influence on the bonding **PTZ** group, and the DA1 and DA2 undergo noticeable fluctuation with varying the environment.

Further, we have simulated the DA1 and DA2 variations in TOL solvent (Figure 3c). The boxes containing two hundred solvents and five or thirty-five target molecules are defined. The calculated results indicate that the DA1 and DA2 of box with thirty-five target molecules undergo much smaller fluctuation than that of box with five target molecules. Especially, for **DPS-PTZ**, the DA1 values of box with thirty-five approach to be horizontal in some time period, demonstrating that the dihedral angle between donor and acceptor is sensitive to the surrounding environment and has a smaller fluctuation with increasing number of target molecules. In polar solvent, the rotatable D-A bond has a better flexibility. However, in the

aggregate state, the local environment is less polar and restrict the twist of D-A bond. Studies indicate that the case of doped in thin film is similar to the low polar solvent environment. Taking the box with two hundred solvents and thirty-five target molecules as example, the DA1 and DA2 of **SF2C** and **SFPC** in TOL fluctuate in a great degree. On the contrary, the DA1 and DA2 of **DPS-PTZ** experience small fluctuations in low polar solvent, suggesting the **PTZ** twist is restricted. The molecular dynamic investigation indicates that the **PTZ** of **DPS-PTZ** in thin film is suppressed to twist and results to AIE property.

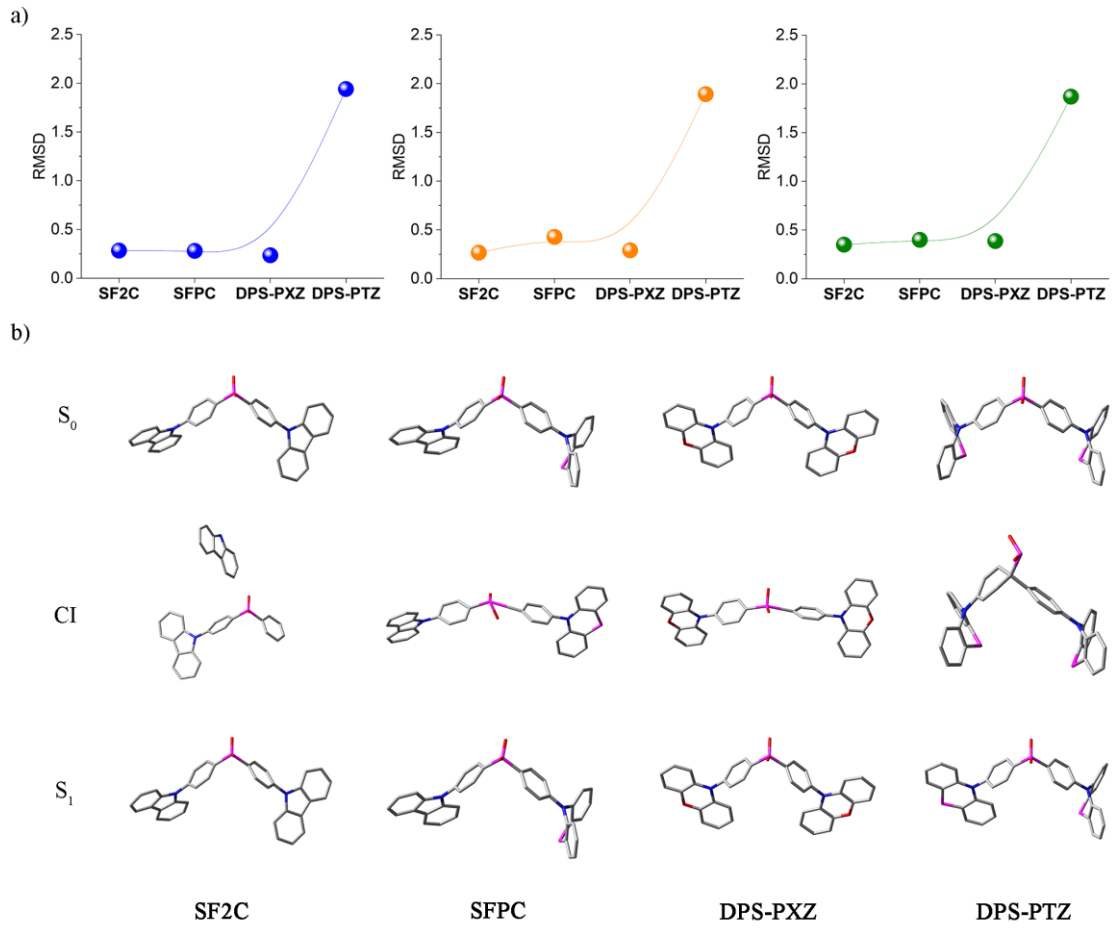

Figure 4. (a) RMSD values between S_0 and S_1 for **SF2C**, **SFPC**, **DPS-PXZ** and **DPS-PTZ** in TOL. (b) The optimized S_0, C1 and S_1 structures of **SF2C**, **SFPC**, **DPS-PXZ** and **DPS-PTZ** in TOL.

It is recognized that the AIE characteristic is attributed to the rotation restriction in the aggregate state. Next, a comparison between S_0 and S_1 geometries in different solvents is discussed. Smaller RMSD imply smaller structural changes during the

electron excited-state relaxation process. In Figure 4a, compared to **SF2C**, **SFPC** and **DPS-PXZ**, the RMSD values of **DPS-PTZ** are relatively large. The geometric comparison indicates that **PTZ** twist of **DPS-PTZ** is noticeably increased. That is, the non-radiative decay of **DPS-PTZ** is huge, but will be suppressed in the aggregate environment demonstrated by dynamic result, leading to AIE characteristic. The combination of molecular dynamics study and quantum calculation suggests that the AIE property of **DPS-PTZ** is originated from the restriction of **PTZ** in the aggregate state.

We further to optimize the S_0/S_1 CI structures of **SF2C**, **SFPC**, **DPX-PXZ** and **DPS-PTZ** in TOL using ORCA program. For **SF2C**, **SFPC** and **DPX-PXZ**, the S_0 and S_1 structures are quite similar confirmed by the small RMSD values (Figure 4). In generally, the **Cz** is stable, but the **Cz** of **SF2C** in CI structure happens to dissociate, indicating that the CI structure of **SF2C** is unreasonable. The bonding **PTZ** of **SFPC** is planar structure in CI configuration. For the CI structure of **SFPC**, the **PTZ** group change from the bonding configuration to the planar configuration. For **DPS-PXZ**, the structures of CI, S_0 and S_1 are very similar with almost vertical donor and acceptor groups and just have different C-S-C degree. Compared to the S_0 and S_1, the C-S-C of CI structure shows a greater angle. Therefore, the CI structure of **DPS-PXZ** is easy to realize via twisting **PXZ** when it is in loose solvent environment and further to S_0 by non-radiative way. However, when the target molecules are in an aggregate state, the CI structure is difficult to realize due to the suppression of C-S-C twist. The S_1 state is fluorescence emitting. That explain the original reason for AIE property for **DPS-PXZ**. Besides, there is large differences between S_0 and S_1 for **DPS-PTZ**. The **PTZ** group of **DPS-PTZ** in S_1 structure is planar, and the obtained CI structure is unreasonable. As a result, the CI structure of **DPS-PTZ** is impossible to achieve.

4. Conclusions

In summary, the purpose of this work was to discover the original aggregation-induced emission (AIE) mechanisms of phenoxazine (**PXZ**) and phenothiazine (**PTZ**) groups. The thermally activated delayed fluorescence (TADF)

property of four molecules were demonstrated by small singlet-triplet energy splitting (ΔE_{ST}) and large spin-orbital coupling (SOC) constant. Besides, we found that the failure of minimum energy crossing point (MECP) structure is beneficial for ensuring the triplet state (T_1) population and facilitating the reverse intersystem crossing (RISC) from T_1 to the singlet state (S_1) for all molecules. The ground-state (S_0) structures of **SF2C** and **DPS-PXZ** are almost unchanged in TOL, THF and DMSO solvents because that **PXZ** group possesses the planar and rigid configuration, but the **SFPC** experiences a quite remarkable change with ranging solvent polarity due to the bonding structure for **PTZ** group. The RMSD values between S_0 and S_1 of **SF2C**, **SFPC** and **DPS-PXZ** are quite small. However, the RMSD values of **DPS-PTZ** are relatively great. According the geometric comparison, we found that the **PTZ** twist is noticeably increased. That is, the non-radiative decay of **DPS-PTZ** is huge and will be suppressed easily in the aggregate environment, leading to AIE characteristic. The combination of molecular dynamics study and quantum calculation suggest that the AIE property of **DPS-PTZ** is originated from the restriction of **PTZ** group in the aggregate state. In the thin film, the surrounding environment restrict the **PTZ** twist, decrease the non-radiative decay and lead to the AIE property for **DPS-PTZ**. The density functional result indicates that the CI structure of **DPS-PXZ** is easy to realize via twisting **PXZ** when it is in loose solvent environment and further to S_0 by non-radiative way. In an aggregate state, the CI structure of **DPS-PXZ** is difficult to realize due to the suppression of C-S-C twist, and the S_1 state is fluorescence emitting. The CI structure forming of **DPS-PXZ** is the key factor for AIE property. Discovering the wording mechanism is beneficial for providing design guidelines for the development of new AIE systems for new practical applications.

Acknowledge

The authors gratefully acknowledge financial support from the National Natural Science Foundation of China (51902124), Department of Education of Jilin Province and Technology Research Projects (JJKH20220179KJ).

References

[1] C.W. Tang, S.A. VanSlyke, Organic electroluminescent diodes, Applied Physics Letters, 51 (1987) 913-915.
[2] H. Uoyama, K. Goushi, K. Shizu, H. Nomura, C. Adachi, Highly efficient organic light-emitting diodes from delayed fluorescence, Nature, 492 (2012) 234-238.
[3] Q. Zhang, B. Li, S. Huang, H. Nomura, H. Tanaka, C. Adachi, Efficient blue organic light-emitting diodes employing thermally activated delayed fluorescence, Nature Photonics, 8 (2014) 326-332.
[4] H. Kaji, H. Suzuki, T. Fukushima, K. Shizu, K. Suzuki, S. Kubo, T. Komino, H. Oiwa, F. Suzuki, A. Wakamiya, Y. Murata, C. Adachi, Purely organic electroluminescent material realizing 100% conversion from electricity to light, Nature Communications, 6 (2015) 8476.
[5] Y. Chen, J.W.Y. Lam, R.T.K. Kwok, B. Liu, B.Z. Tang, Aggregation-induced emission: fundamental understanding and future developments, Materials Horizons, 6 (2019) 428-433.
[6] G. Méhes, H. Nomura, Q. Zhang, T. Nakagawa, C. Adachi, Enhanced Electroluminescence Efficiency in a Spiro-Acridine Derivative through Thermally Activated Delayed Fluorescence, Angewandte Chemie International Edition, 51 (2012) 11311-11315.
[7] J. Luo, Z. Xie, J.W.Y. Lam, L. Cheng, H. Chen, C. Qiu, H.S. Kwok, X. Zhan, Y. Liu, D. Zhu, B.Z. Tang, Aggregation-induced emission of 1-methyl-1,2,3,4,5-pentaphenylsilole, Chemical Communications, (2001) 1740-1741.
[8] Y. Hong, J.W.Y. Lam, B.Z. Tang, Aggregation-induced emission: phenomenon, mechanism and applications, Chemical Communications, (2009) 4332-4353.
[9] Z. Zhao, H. Zhang, J.W.Y. Lam, B.Z. Tang, Aggregation-Induced Emission: New Vistas at the Aggregate Level, Angewandte Chemie International Edition, 59 (2020) 9888-9907.
[10] J. Mei, N.L.C. Leung, R.T.K. Kwok, J.W.Y. Lam, B.Z. Tang, Aggregation-Induced Emission: Together We Shine, United We Soar!, Chemical Reviews, 115 (2015) 11718-11940.
[11] Q. Peng, Y. Yi, Z. Shuai, J. Shao, Toward Quantitative Prediction of Molecular Fluorescence Quantum Efficiency: Role of Duschinsky Rotation, Journal of the American Chemical Society, 129 (2007) 9333-9339.
[12] Z. Zhao, P. Lu, J.W.Y. Lam, Z. Wang, C.Y.K. Chan, H.H.Y. Sung, I.D. Williams, Y. Ma, B.Z. Tang, Molecular anchors in the solid state: Restriction of intramolecular rotation boosts emission efficiency of luminogen aggregates to unity, Chemical Science, 2 (2011) 672-675.
[13] Z. Yang, W. Qin, N.L.C. Leung, M. Arseneault, J.W.Y. Lam, G. Liang, H.H.Y. Sung, I.D. Williams, B.Z. Tang, A mechanistic study of AIE processes of TPE luminogens: intramolecular rotation vs. configurational isomerization, Journal of Materials Chemistry C, 4 (2016) 99-107.
[14] N.L.C. Leung, N. Xie, W. Yuan, Y. Liu, Q. Wu, Q. Peng, Q. Miao, J.W.Y. Lam, B.Z. Tang, Restriction of Intramolecular Motions: The General Mechanism behind Aggregation-Induced Emission, Chemistry – A European Journal, 20 (2014) 15349-15353.
[15] Y. Ren, J.W.Y. Lam, Y. Dong, B.Z. Tang, K.S. Wong, Enhanced Emission Efficiency and Excited State Lifetime Due to Restricted Intramolecular Motion in Silole Aggregates, The Journal of Physical Chemistry B, 109 (2005) 1135-1140.
[16] W.-L. Ding, X.-L. Peng, G.-L. Cui, Z.-S. Li, L. Blancafort, Q.-S. Li, Potential-Energy Surface and Dynamics Simulation of THBDBA: An Annulated Tetraphenylethene Derivative Combining Aggregation-Induced Emission and Switch Behavior, ChemPhotoChem, 3 (2019) 814-824.

[17] B.-K. An, J. Gierschner, S.Y. Park, π-Conjugated Cyanostilbene Derivatives: A Unique Self-Assembly Motif for Molecular Nanostructures with Enhanced Emission and Transport, Accounts of Chemical Research, 45 (2012) 544-554.
[18] H. Naito, K. Nishino, Y. Morisaki, K. Tanaka, Y. Chujo, Solid-State Emission of the Anthracene-o-Carborane Dyad from the Twisted-Intramolecular Charge Transfer in the Crystalline State, Angewandte Chemie International Edition, 56 (2017) 254-259.
[19] Y. Qian, M.-M. Cai, L.-H. Xie, G.-Q. Yang, S.-K. Wu, W. Huang, Restriction of Photoinduced Twisted Intramolecular Charge Transfer, ChemPhysChem, 12 (2011) 397-404.
[20] R. Hu, S. Li, Y. Zeng, J. Chen, S. Wang, Y. Li, G. Yang, Understanding the aggregation induced emission enhancement for a compound with excited state intramolecular proton transfer character, Physical Chemistry Chemical Physics, 13 (2011) 2044-2051.
[21] M. Chen, L. Li, H. Nie, J. Tong, L. Yan, B. Xu, J.Z. Sun, W. Tian, Z. Zhao, A. Qin, B.Z. Tang, Tetraphenylpyrazine-based AIEgens: facile preparation and tunable light emission, Chemical Science, 6 (2015) 1932-1937.
[22] Z. Zhao, B. He, B.Z. Tang, Aggregation-induced emission of siloles, Chemical Science, 6 (2015) 5347-5365.
[23] Y. Li, A. Shao, Y. Wang, J. Mei, D. Niu, J. Gu, P. Shi, W. Zhu, H. Tian, J. Shi, Morphology-Tailoring of a Red AIEgen from Microsized Rods to Nanospheres for Tumor-Targeted Bioimaging, 28 (2016) 3187-3193.
[24] C.Y.Y. Yu, H. Xu, S. Ji, R.T.K. Kwok, J.W.Y. Lam, X. Li, S. Krishnan, D. Ding, B.Z. Tang, Mitochondrion-Anchoring Photosensitizer with Aggregation-Induced Emission Characteristics Synergistically Boosts the Radiosensitivity of Cancer Cells to Ionizing Radiation, 29 (2017) 1606167.
[25] J. Zhang, S. Ma, H. Fang, B. Xu, H. Sun, I. Chan, W. Tian, Insights into the origin of aggregation enhanced emission of 9,10-distyrylanthracene derivatives, Materials Chemistry Frontiers, 1 (2017) 1422-1429.
[26] J. Zhang, H. Zhang, J.W.Y. Lam, B.Z. Tang, Restriction of Intramolecular Motion(RIM): Investigating AIE Mechanism from Experimental and Theoretical Studies, Chemical Research in Chinese Universities, 37 (2021) 1-15.
[27] J. Chen, C.C.W. Law, J.W.Y. Lam, Y. Dong, S.M.F. Lo, I.D. Williams, D. Zhu, B.Z. Tang, Synthesis, Light Emission, Nanoaggregation, and Restricted Intramolecular Rotation of 1,1-Substituted 2,3,4,5-Tetraphenylsiloles, Chemistry of Materials, 15 (2003) 1535-1546.
[28] N.B. Shustova, B.D. McCarthy, M. Dincă, Turn-On Fluorescence in Tetraphenylethylene-Based Metal–Organic Frameworks: An Alternative to Aggregation-Induced Emission, Journal of the American Chemical Society, 133 (2011) 20126-20129.
[29] Q. Yu, J. Zhang, J.W.Y. Lam, D. Yang, J. Sun, B.Z. Tang, Tunable Room Temperature Phosphorescence in Heavy-Atom-Free Metal–Organic Frameworks by Ligand Functionalization, ACS Materials Letters, 5 (2023) 2691-2699.
[30] H. Zou, L. Liu, S. Zhang, X. Miao, L. Ying, W. Deng, Y. Cao, Different Stepwise Growth Mechanism of AIE-Active Tetraphenylethylene-Functionalized Metal–Organic Frameworks on Au(111) and Cu(111) Surfaces, The Journal of Physical Chemistry Letters, 14 (2023) 489-498.
[31] B. He, S. Ye, Y. Guo, B. Chen, X. Xu, H. Qiu, Z. Zhao, Aggregation-enhanced emission and efficient electroluminescence of conjugated polymers containing tetraphenylethene units, Science China Chemistry, 56 (2013) 1221-1227.

[32] B.-R. Gao, H.-Y. Wang, Y.-W. Hao, L.-M. Fu, H.-H. Fang, Y. Jiang, L. Wang, Q.-D. Chen, H. Xia, L.-Y. Pan, Y.-G. Ma, H.-B. Sun, Time-Resolved Fluorescence Study of Aggregation-Induced Emission Enhancement by Restriction of Intramolecular Charge Transfer State, The Journal of Physical Chemistry B, 114 (2010) 128-134.
[33] R. Hu, E. Lager, A. Aguilar-Aguilar, J. Liu, J.W.Y. Lam, H.H.Y. Sung, I.D. Williams, Y. Zhong, K.S. Wong, E. Peña-Cabrera, B.Z. Tang, Twisted Intramolecular Charge Transfer and Aggregation-Induced Emission of BODIPY Derivatives, The Journal of Physical Chemistry C, 113 (2009) 15845-15853.
[34] J. Guo, X.-L. Li, H. Nie, W. Luo, S. Gan, S. Hu, R. Hu, A. Qin, Z. Zhao, S.-J. Su, B.Z. Tang, Achieving High-Performance Nondoped OLEDs with Extremely Small Efficiency Roll-Off by Combining Aggregation-Induced Emission and Thermally Activated Delayed Fluorescence, Advanced Functional Materials, 27 (2017) 1606458.
[35] J. Liu, H. Zhang, L. Hu, J. Wang, J.W.Y. Lam, L. Blancafort, B.Z. Tang, Through-Space Interaction of Tetraphenylethylene: What, Where, and How, Journal of the American Chemical Society, 144 (2022) 7901-7910.
[36] S. Xu, T. Liu, Y. Mu, Y.-F. Wang, Z. Chi, C.-C. Lo, S. Liu, Y. Zhang, A. Lien, J. Xu, An Organic Molecule with Asymmetric Structure Exhibiting Aggregation-Induced Emission, Delayed Fluorescence, and Mechanoluminescence, 54 (2015) 874-878.
[37] Z. Xie, C. Chen, S. Xu, J. Li, Y. Zhang, S. Liu, J. Xu, Z. Chi, White-Light Emission Strategy of a Single Organic Compound with Aggregation-Induced Emission and Delayed Fluorescence Properties, 54 (2015) 7181-7184.
[38] S. Gan, W. Luo, B. He, L. Chen, H. Nie, R. Hu, A. Qin, Z. Zhao, B.Z. Tang, Integration of aggregation-induced emission and delayed fluorescence into electronic donor–acceptor conjugates, Journal of Materials Chemistry C, 4 (2016) 3705-3708.
[39] I.H. Lee, W. Song, J.Y. Lee, Aggregation-induced emission type thermally activated delayed fluorescent materials for high efficiency in non-doped organic light-emitting diodes, Organic Electronics, 29 (2016) 22-26.
[40] H. Wu, X.-C. Fan, H. Wang, F. Huang, X. Xiong, Y.-Z. Shi, K. Wang, J. Yu, X.-H. Zhang, Conformational isomerization: A novel mechanism to realize the AIE-TADF behaviors, Aggregate, 4 (2023) e243.
[41] X. Wu, C. Gong, X. Jiang, J. Gao, M. Li, R. He, P. Chen, W. Shen, Face-to-face order-packed mode promotes thermally activated delayed fluorescence to achieve stronger aggregation-induced emission, Journal of Science: Advanced Materials and Devices, 7 (2022) 100432.